Design and Performance Assessment of a Prefabricated BIPV/T Roof System Coupled with a Heat Pump

E. D. Rounis[1], Z. Ioannidis[1], R. Dumoulin[1], O. Kruglov[1], A. Athienitis[1], T. Stathopoulos[1]

[1] Centre for Zero Energy Building Studies, Department of Building, Civil and Environmental Engineering, Concordia University, Montreal, Canada

Abstract

This paper describes the design, development and simulated performance of a building integrated photovoltaic/thermal (BIPV/T) roof system, coupled with a water-to-water heat pump. This system is installed on a prefabricated low-energy house, designed for the Solar Decathlon China 2018 contest. The open-loop, air-based BIPV/T roof system is fully integrated and is based on the design of a curtain wall BIPV/T prototype. The preheated air collected by the system is driven through a custom manifold to an air-to-water heat recovery ventilator (HRV) unit which is in turn linked to the cold storage tank of the heat pump. The objective of this paper is to provide insight on the design and performance of fully integrated BIPV/T roof systems and introduce concepts of modular prefabrication of such systems. The performance of the coupled BIPV/T-heat pump system was modelled in TRNSYS.

Keywords: Building-integrated photovoltaic/thermal, prefabricated net-zero house, modelling, TRNSYS.

1. Introduction

Integration of photovoltaic/thermal (PV/T) systems with the building envelope is a crucial part of the net-zero energy building concept. An active envelope system becomes the energy generating part of the building, while the integration itself entails such benefits as superior aesthetics and increased cost effectiveness due to the replacement of common envelope materials (Yang and Athienitis, 2016). Open-loop, air-based BIPV/T systems have an air channel behind the photovoltaic (PV) modules which serves both as a means of cooling the PV modules and of collecting preheated fresh air. Although there are several studies on BIPV/T systems (Chen et al, 2010; Athienitis et al 2010; Zogou and Stapountzis, 2011) and stand-alone PV/T systems (Wolf, 1976; Florschuetz, 1979; Hegazy, 2000; Hussain et al, 2015, Tonui and Tripanagnostopoulos, 2007), such systems currently hold the smallest share of PV applications. This can be attributed to two main factors, namely, the lack of a BIPV/T design and performance standard and the adherence of the engineering community to known building practices.

This study introduces a novel BIPV/T roof system (Fig. 1) coupled with a two-tank, water-to-water heat pump, installed on a prefabricated low-energy/net-zero residential building. The building, also known as the "Deep Performance Dwelling" or "DPD", is of a row house typology with a floor area of 200 m^2 and was designed for the Solar Decathlon China 2018 competition, in Dezhou, China. This system is based upon a BIPV/T curtain wall prototype (Rounis et al, 2017; Kruglov et al, 2017). Several aspects of the design are presented, such as the structural and architectural integration, building envelope considerations, as well as the coupling with an HRV unit via a custom manifold. Concepts of modularity and prefabrication are also discussed.

The coupled system's performance was modelled using TRNSYS and simulated for the local climate of Dezhou, China. The results focus on the electrical and thermal output of the system, both in terms of heat recovery at the air collector's end and heat delivered at the mechanical system. The main goals of this investigation are to provide insight on the design and performance of BIPV/T roof systems intended for full integration, as well as analyze thermal utilization strategies through numerical investigation of the coupled BIPV/T-heat pump system.

2. Overall building and mechanical system description

The Deep Performance Dwelling (DPD) (Figure 1) is a two-story building of the row house typology, with a foot print of 116 m^2 and a total heated space of 200 m^2. It was designed by Team Montreal for the 2018 Solar Decathlon

doi:10.18086/eurosun2018.02.06 Available at http://proceedings.ises.org

Competition, held in Dezhou, China. The building was designed to represent one unit of attached row houses, a residential building typology very common in dense urban settings. The design of the house included three main components, namely, passive design with a highly insulated, air-tight envelope to minimize the energy demand for conditioning, on-site energy generation with integrated systems and electrical and thermal storage for optimal use of that energy.

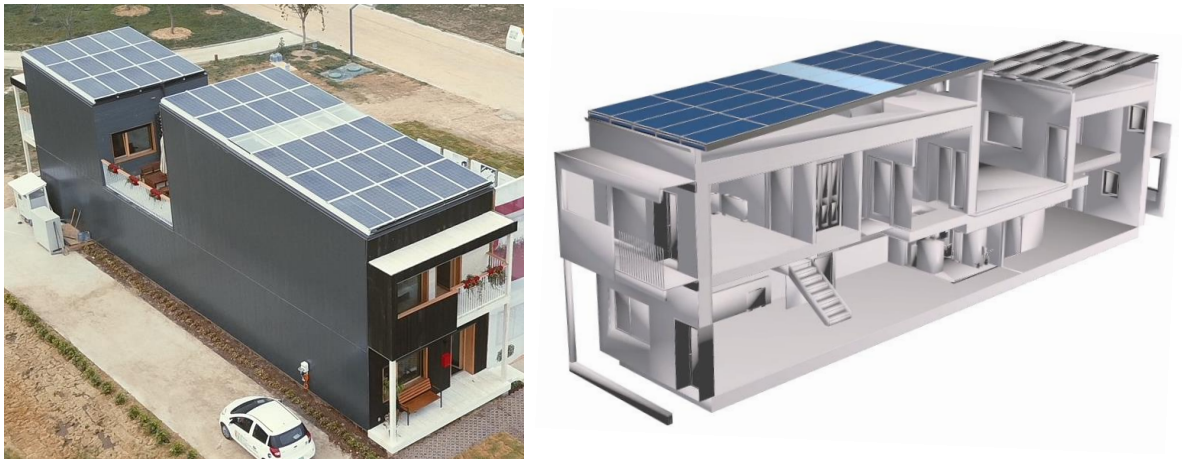

Fig. 1: The Deep Performance Dwelling (DPD). Installed on the back roof is a building integrated photovoltaic system (BIPV) and on the front roof a building integrated photovoltaic /thermal (BIPV/T) system with an integrated skylight.

2.1 Passive design and HVAC

The passive design reduces the heating energy demand of the house by 80% on average versus poorly insulated housing. This is achieved by the highly insulated walls (RSI 10.4) and roof (RSI 15.3), as well as the high-performance triple-glazed windows (RSI 1) and skylight system.

An important aspect of the design process was the concept of prefabrication and modularity. The building envelope (walls, roof) was prefabricated in modules which were assembled on site with the use of a crane. This was partly used for the BIPV and BIPV/T roofs of the building, the construction of which combined pre-assembled parts of the frame with on-site assembly.

Heating and cooling is provided by four local, two-pipe fan-coil units, one for each primary thermal zone of the house, which can operate in independent modes. These units are supplied with water by two 450-litre thermal storage tanks, one hot and one cold, depending on the demand of each zone. The two tanks temperature is maintained at desired setpoints (below 7^{o}C for the cold tank and 35^{o}C for the hot tank in summer mode and over 0^{o}C for the cold tank and 45^{o}C for the hot tank in winter mode) via a 2-ton water to water heat pump. Domestic hot water is supplied by a 190-litre hybrid HP water heater, which utilizes the heat produced by the equipment in the mechanical room by storing it in the tank via an air to water heat pump, also controlling the temperature of the room itself. A high-efficiency Energy Recovery Ventilation unit is used for heat and moisture recovery during the winter and dehumidification during the summer.

2.2 Energy generation and storage

An air-based, open-loop Building Integrated Photovoltaic/Thermal (BIPV/T) system is installed on the front roof of the house and a Building Integrated Photovoltaic (BIPV) system is installed on the back roof, as demonstrated in Figure 1. During winter, the thermal energy harvested from the BIPV/T system is stored on the cold tank of the two tank-heat pump system via an air-to-water heat exchanger unit. The same unit is used during the summer to remove heat from the hot tank and release it to the ambient environment. This results in reduction of the temperature difference of the two tanks in both cooling and heating mode and thus increasing the water-to-water heat pump's coefficient of performance (COP).

Furthermore, a 10-kWh lithium-ion battery serves as electrical storage, which can both provide back-up in case of power outages, as well as assist the grid in the peak power demand periods. Figure 2 demonstrates a simplified schematic of the mechanical system.

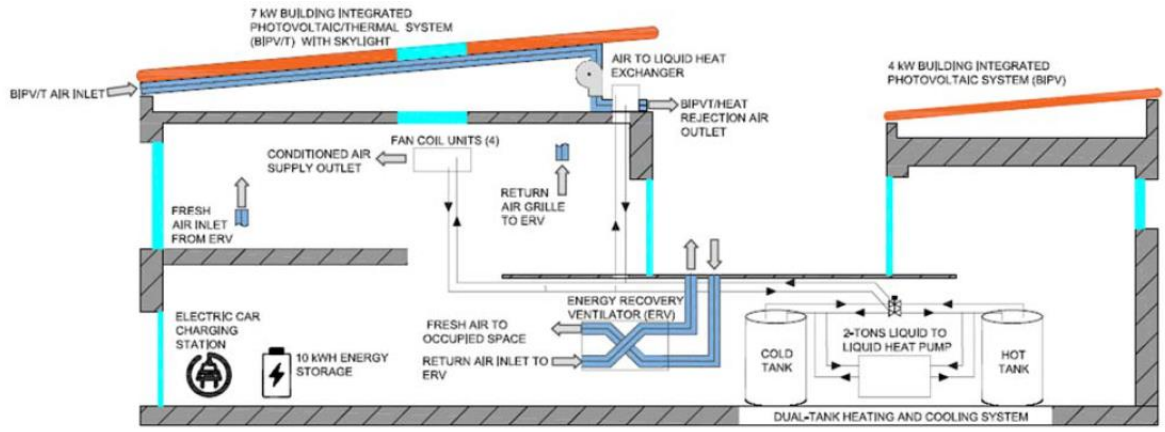

Fig. 2: Simplified schematic of the mechanical system of the DPD

3. BIPV/T and BIPV systems

3.1. BIPV/T Curtain Wall prototype

A BIPV/T curtain wall prototype designed, developed and tested at Concordia University in Montreal, served as the basis for the design of the BIPV/T system implemented in the DPD. The development of the prototype was done within the scope of implementing common building techniques in the design of BIPV/T systems, which could lead to the standardization of such systems and wider application in the market.

For the development of the prototype, the curtain wall concept was adopted and modified in order to accommodate the air flow of the system. The design and development of the prototype is documented in detail in Rounis et al (2017) and Kruglov et al (2017). The prototype (Figure 3) consists of an aluminum curtain wall frame with commercial mullion extrusions, frameless PVs fixed on the frame with Pressure plates as well as point supports (brackets) and rigid insulation supported by a typical aluminum back pan. The experimental prototype also features an extra air intake (inlet) as a method of enhancing heat extraction from the PV by disrupting the thermal boundary layer formed on the inner PV surface.

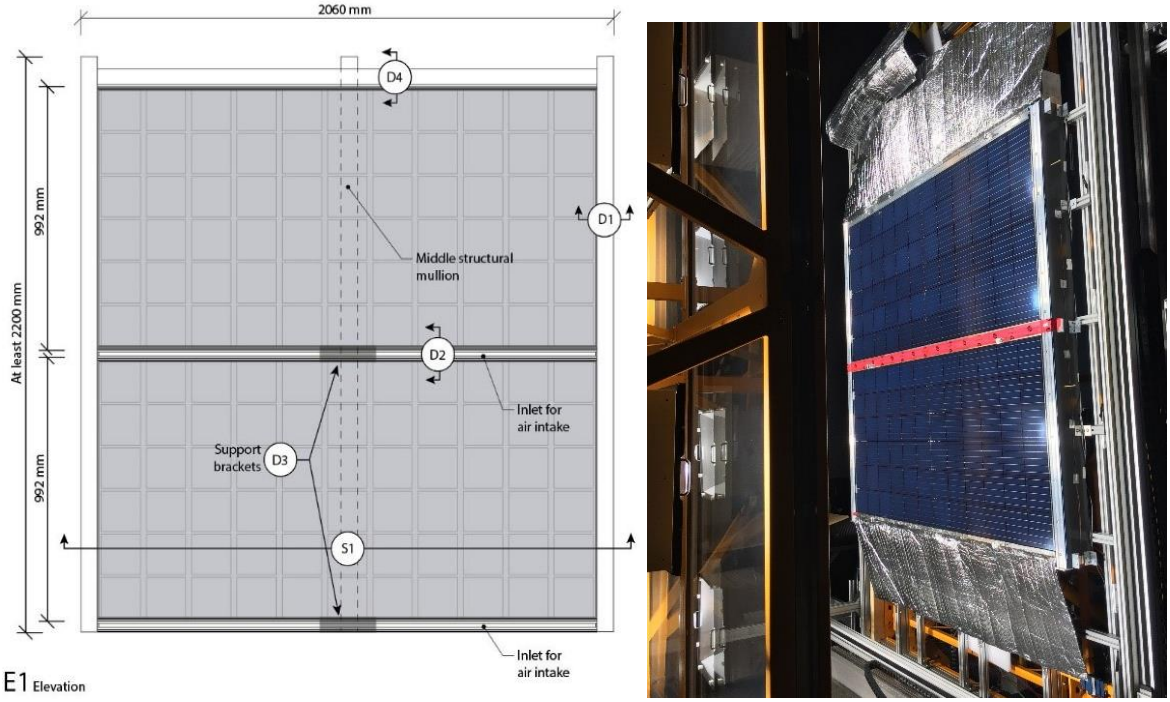

Fig. 3: Experimental BIPV/T curtain wall prototype design (left) and testing (right)

The prototype's construction features the curtain wall stick built method of assembly. The potential of designing a unitized system with a modular approach is currently under investigation. Modularization of BIPV/T can further

encompass the system's standardization, as well as extend its range of application for both new buildings and retrofits.

3.2 BIPV/T and BIPV roof systems of the DPD

The curtain wall concept was adopted for the integrated roof systems of the DPD. The front and back roof of the DPD employ a BIPV/T and a BIPV system respectively. Both systems incorporate a curtain wall aluminum framing system. The following section focuses on the features of the open-loop BIPV/T system of the front roof.

The BIPV/T consists of 25 CS6X-310W PV modules, forming a 7.75 kW peak power system, with an integrated skylight system supported by a curtain wall frame. The frame consists of vertical and horizontal structural elements (mullions), of which the horizontal has a shallow height in order to allow the air flow for the air channels formed between the vertical. Semi-rigid insulation is set at a distance of 10 cm from the PV surface and supported by aluminum back pans at the rear side of the frame. Five air channels are thus formed (5 PV modules and a glazing unit for each channel) as shown on the structural breakdown of the BIPV/T system in Figure 4.

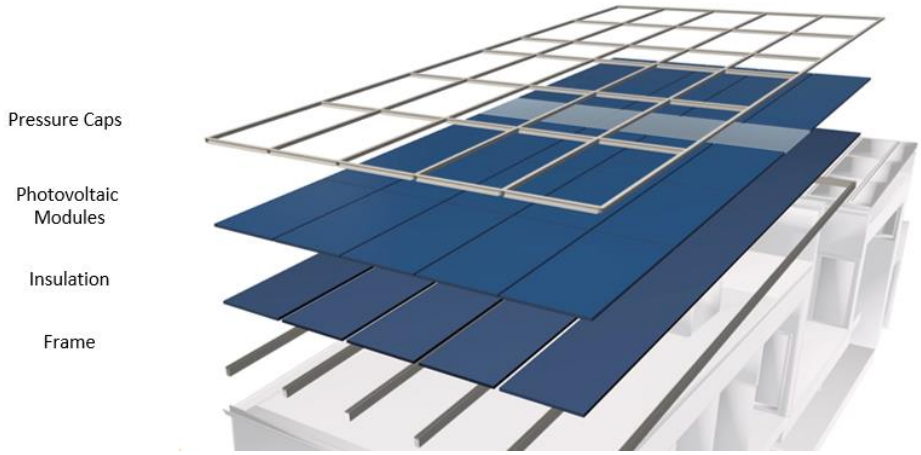

Fig. 4: BIPV/T roof breakdown

The curtain wall technique allowed for an easy incorporation of a skylight system that allows natural daylight in the living space bellow. The latter is a challenge for row houses, especially when incorporating a PV roof. The skylight consists of a double-glazing unit on top and a single glazing on the bottom, allowing for a continuous air channel. Figure 5 showcases the seamless architectural integration of the PV and the skylight.

Fig. 5: Finished BIPV/T roof with integrated skylight

The BIPV system of the back roof consists of 15 CS6X-310W PV modules (4.65 kW peak power), also employing a curtain wall frame. Its design is simpler since it is comprised only of the PV modules supported by the frame, without the air channel.

Both roof systems have a 5º tilt which to meet the competition's maximum height requirements, although the optimal tilt would closer to 40º in order to maximize incident solar irradiation annually and avoid snow accumulation. The effect of an optimal and a non-optimal system tilt is discussed in section 4.2.

3.3 Thermal operation

At the top of the BIPV/T system a custom manifold was connected via two take-offs per channel to ensure flow uniformity for all channels. The manifold (Figure 6) was previously balanced at Concordia University via manually operated dampers installed at each take off.

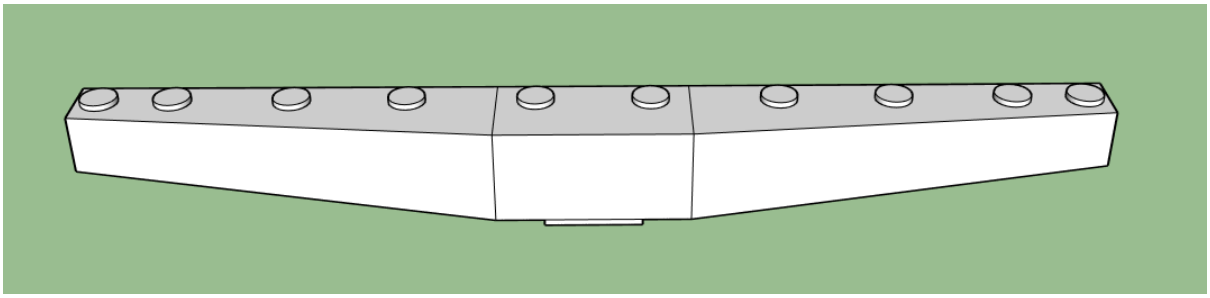

Fig. 6: The BIPV/T manifold (two take-offs per channel)

The main duct of the manifold is connected to an air-to-water heat exchanger. The water loop of the heat exchanger is connected to the two-tank heat pump system. In winter mode, the heat transferred by the pre-heated air from the BIPV/T system to the water loop, is then stored in the cold tank to increase its temperature. During summer mode, the BIPV/T system is naturally ventilated via dumpers, while the heat exchange unit is now used to cool the hot tank of the system. Figure 7 demonstrates a schematic of the connection between the BIPV/T and the mechanical system of the building.

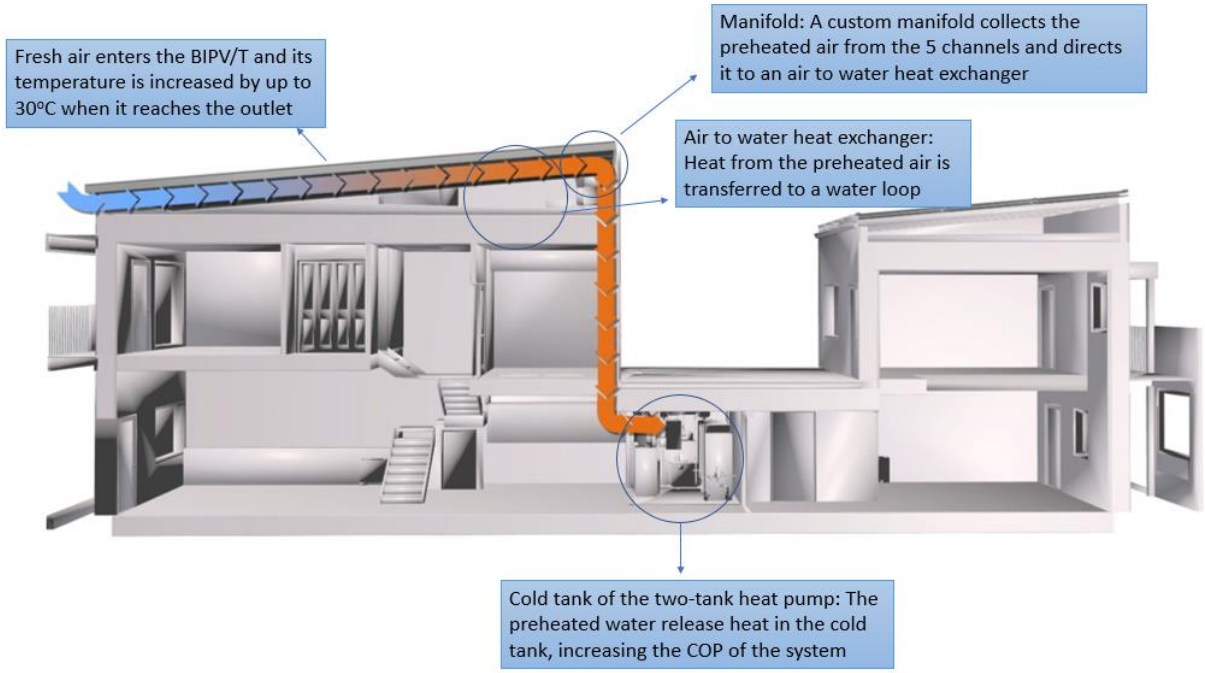

Fig. 7: Integrattion of the BIPV/T and the mechanical system

4. Modelling and simulations

The performance of the BIPV/T system in conjunction with the mechanical system was evaluated using the software TRNSYS. The following section summarizes the modelling assumptions and methodology, as well as results on the thermal performance of the system during winter for various flow rates of the air channel and of the water loop.

4.1 BIPV/T modelling

The BIPV/T modelling was done in TRNSYS using a modified version of Type 567 from the Thermal Energy Systems Specialists (TESS) libraries (TESSLibs 17), interfacing with Type 56 for multi-zone buildings. A semi-conditioned zone was defined between the building and the BIPV/T system, with the latter set as a boundary of

that zone.

The BIPV/T energy balance has been well documented in literature (Candanedo et al, 2011; Chen et al, 2010; Yang and Athienitis, 2014) and the resulting governing equations are solved in an iterative manner in TRNSYS, using initial guesses for the PV and back surface temperatures. A typical energy balance for a photovoltaic thermal system is presented in Figure 8 in the form of a thermal network.

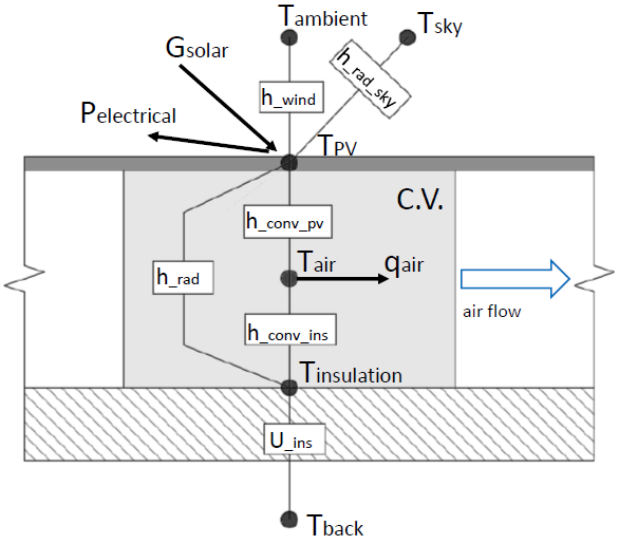

Fig. 8: Finished BIPV/T roof with integrated skylight

Where $T_{ambient}$, T_{sky}, T_{PV}, T_{air}, $T_{insulation}$ and T_{back} (°C) are the temperatures of the ambient, sky, PV, cavity air, insulation surface and back room respectively; $h_{\_rad\_sky}$, $h_{\_rad}$ (W/m^2 K) are the coefficients for radiative heat exchange between the PV and the sky and PV and the insulation respectively, $h_{\_conv\_PV}$, $h_{\_conv\_ins}$ (W/m^2 K) are the convective heat transfer coefficients inside the air cavity, U_{ins} (W/m^2 K) is the insulation u-value, G_{solar} (W/m^2) is the insident solar irradiation, $P_{electrical}$ (W/m^2) is the electrical power generated by the PV and q_{air} (W/m^2) is the rate of heat transfer in the cavity air stream.

Type 567 (and generally BIPV/T types in TRNSYS) assumes a single convective heat transfer coefficient (CHTC or h_{conv}) for top (PV) and bottom (insulation) surfaces of the air channel, evaluated using the Nusselt number, which in turn is calculated depending the flow regime. The CHTC (h_{conv}) is then calculated as follows:

$$h_{conv} = \frac{Nu \cdot k}{L} \qquad \text{(eq. 1)}$$

Where k (W/m K) is the thermal conductivity of the fluid and L (m) the characteristic length, which in the case of non-circular pipes is the hydraulic diameter of the air channel, $D_h = 4 \cdot A_c / p$, where A_c (m^2) is the channel cross-sectional area and p (m) its perimeter.

For the case of forced, turbulent flow, the Nusselt number (Nu) is calculated according to the Dittus-Boelter equation (eq. 2).

$$\overline{Nu} = 0.023 Re^{0.8} Pr^{n} \qquad \text{(eq. 2)}$$

Where Re is the Reynolds number, which indicates the flow regime, Pr is the Prandtl number of air and n is an exponent equal to n=0.3 when heat is transferred from the fluid to the duct wall and n=4 when heat is transferred from the surface to the fluid.

The Dittus-Boelter equation has been developed for smooth duct with developed turbulent flow (Candanedo et al, 2011). It may, therefore, underestimate convective heat transfer in the air channel of a BIPV/T, since the channel is not smooth due to frame protrusions and the surface roughness and it may also neglect the entrance effects, where heat exchange is highest at the entrance region of the flow. This correlation was modified within the TRNSYS type and channel convection was evaluated by the empirical correlations developed and validated by Chen et al (2010) for a fool scale roof BIPV/T system (eq. 3).

$$h_{conv} = \begin{cases} 10.2 & if\ 0.4 \le v_{fluid} \le 0.6\ m/s \\ 12 \cdot v_{fluid} + 3 & if\ v_{fluid} > 0.6\ m/s \end{cases} \quad \text{(eq. 3)}$$

Where v_{fluid} (m/s) is the average air speed within the BIPV/T channel. Equation (3) also assumes a single value for the top and bottom convective heat transfer coefficients of the channel, as well as an average value for the whole channel length. The heat collected by the system on the air side is calculated as follows:

$$q_{thermal} = \dot{m} \cdot C_p \cdot \Delta T \quad \text{(eq. 4)}$$

Where $q_{thermal}$ (W) is the heat recovered from the BIPV/T system, C_p is the specific heat capacity of air and ΔT is the air temperature difference between the inlet and outlet of the BIPV/T air channel.

The thermal efficiency ($\eta_{thermal}$) on the air side (outlet of the BIPV/T system) is defined as the ratio of the heat recovered ($q_{thermal}$) over the total incident solar irradiation. The rest of the equipment, namely, the heat exchanger, the water loop and the two-tank heat pump system have been modelled as black boxes in TRNSYS. The thermal efficiency at the water side (heat delivered to the cold tank), is defined as the ratio of the heat delivered to the cold tank over the total incident irradiation on the BIPV/T surface. Heat is delivered to the cold tank only when the temperature of water in the water loop is higher than that of the water in the cold tank.

Regarding the electrical output of the system, this is calculated as a function of the PV temperature (Kaiser et al, 2014; Tonui and Tripanagnostopoulos, 2006; Anderson et al, 2008; Skoplaki and Palyvos, 2009). The electrical efficiency, η_{elec}, is calculated as follows:

$$\eta_{elec} = \eta_o \cdot [1 - \beta \cdot (T_{PV} - T_{STC})] \quad \text{(eq. 5)}$$

Where η_{ref} is the reference efficiency of the PV module at standard testing conditions (STC), β is the temperature coefficient of the PV, T_{PV} is the average PV module temperature and T_{STC} is a reference PV temperature of 25ºC (STC).

4.2 Simulations and results

A numerical investigation was carried out in TRNSYS regarding the thermal performance of the combined BIPV/T-heat pump system, for a cold sunny day in Dezhou, China. For the selected day, simulations were run to investigate the thermal output for the air side (heat collected by the air in the air channel of the BIPV/T) and the water side (the end heat delivered by the water loop to the cold tank). Two roof tilts were considered, namely the 5º tilt the house was designed with for the competition and a 45º slope which would be near optimal for maximum annual incident solar irradiation over the PV surface. Finally, four total mass flow rates were considered, corresponding to four average velocities in the air channel, namely, 0.25 m/s, 0.5 m/s, 0.75 m/s and 1 m/s.

Figures 9a and 9b demonstrate the heat recovery at the air and water side against average air velocity in the air channel, for the actual roof slope of 5º and the near optimal roof slope of 40º respectively. Figures 10a and 10b show the corresponding thermal efficiency for the two roof slopes.

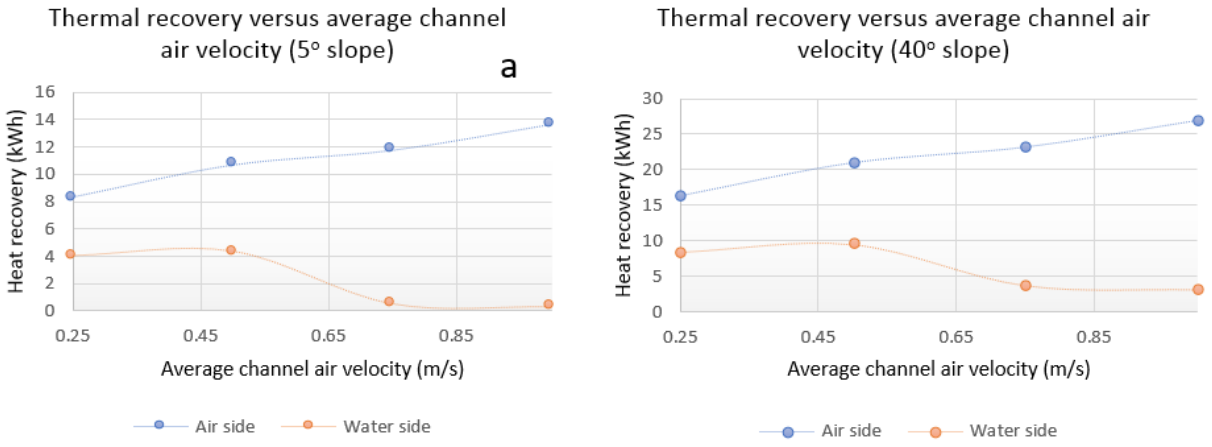

Fig. 9: Thermal recovery versus average air velocity inside the cavity for the air side (air outlet of the BIPV/T) and the water side (delivered to the cold tank) for a. 5º roof slope and b. 40º roof slope

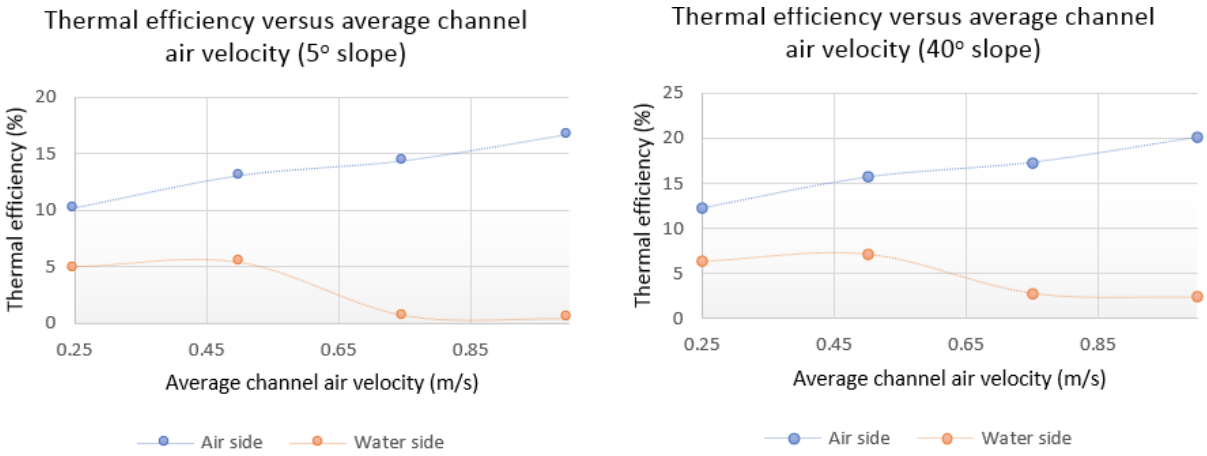

Fig. 10: Thermal efficiency versus average air velocity inside the cavity for the air side (air outlet of the BIPV/T) and the water side (delivered to the cold tank) for a. 5° roof slope and b. 40° roof slope

From the results it can be concluded that increasing the average channel air velocity increases the heat recovered from the BIPV/T, in accordance with previous studies (Bambrook and Sproul, 2012; Yang and Athienitis, 2014; Hegazy, 2000). The thermal efficiency of the BIPV/T can be over 20%, for optimal tilt and for an average air cavity velocity of 1 m/s. However, in terms of overall heat recovery and end use, which in this case is heat delivered to the cold tank of the two-tank system, maximum airflow is not the optimal. An algorithm could be used to optimize flow rate at any given time, however, the simulations showed that a fixed velocity of 0.5 m/s yields the best results for the heating season, simplifying the controls of the system.

A lower heat transfer rate in the cavity produces more favorable results for this system configuration, since the delivery of useful heat depends on the temperature differential between the cavity air and the fluid in the heat exchanger on the air side and the temperature difference between the fluid and the water in the cold tank on the water side. The useful heat delivered to the cold tank has been calculated to be up to 4 MWh annually.

Finally, the results showcase the importance of the roof slope. Optimizing the roof slope resulted in more than double the amount of useful heat delivered to the system as opposed to the actual building slope. This is also evident in the average monthly electrical and thermal output of the system for the two roof slopes, as demonstrated in Figure 11.

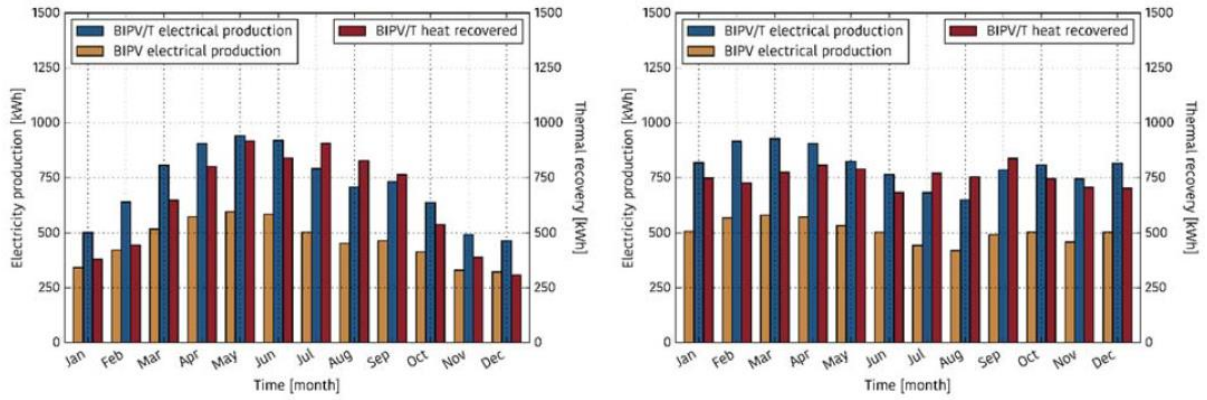

Fig. 11: Monthly electrical and thermal output of the BIPV/T system for a 5° roof slope (left) and a 45° roof slope (right).

It must be noted that the specific way that heat from the BIPV/T was utilized is only one of many potential options and was dictated by construction restrictions and requirements for system compactness. Other options could include preheating of domestic hot water (DHW), as well as a solar heating driven cooling system, such as desiccant cooling, in which cases heat from the BIPV/T could be further exploited even during the cooling season.

5. Summary and Conclusions

In this paper the design, development and simulated performance of a roof BIPV/T system coupled with a water to water heat pump is described. The curtain wall building technique has been adopted as a novel way to implement

BIPV/T systems, which could lead to the standardization of such systems and has the potential for prefabrication and modularization.

The performance of the coupled BIPV/T-heat pump system was modelled in TRNSYS. From the simulated system's performance the following can be concluded:

- The tilt of the BIPV/T system, determined by the building's slope, has a critical effect on its annual electrical and thermal performance.
- Increasing the flow rate in the air cavity produces higher thermal output at the end of the BIPV/T collector, but this can be at the cost of the required temperature for the mechanical system linked to the BIPV/T. The flow rate in the BIPV/T system's cavity must be optimized according to the end use
- Although the thermal efficiency is a common reference for the characterization and comparison of photovoltaic/thermal systems, it is the heat delivered to the actual thermal application that should dictate the design and performance optimization of the system at the collector level.

6. References

Anderson, T.N., Duke, M., Morrison, G.L., Carson, J.K., 2009. Performance of a building integrated photovoltaic/thermal (BIPVT) solar collector. Sol. Energy 83, 445–455. doi:10.1016/j.solener.2008.08.013

Bambara, J., Athienitis, A.K., O'Neill, B., 2011. Design and performance of a photovoltaic/thermal system integrated with transpired collector. ASHRAE Trans. 117, 403–410. doi:10.1016/j.solener.2010.10.008

Bambrook, S.M., Sproul, A.B., 2012. Maximising the energy output of a PVT air system. Sol. Energy 86, 1857–1871. doi:10.1016/j.solener.2012.02.038

Candanedo, L.M., Athienitis, A., Park, K.-W., 2011. Convective Heat Transfer Coefficients in a Building-Integrated Photovoltaic/Thermal System. J. Sol. Energy Eng. 133, 21002. doi:10.1115/1.4003145

Chen, Y., Athienitis, A.K., Galal, K., 2010. Modeling, design and thermal performance of a BIPV/T system thermally coupled with a ventilated concrete slab in a low energy solar house: Part 1, BIPV/T system and house energy concept. Sol. Energy 84, 1892–1907. doi:10.1016/j.solener.2010.06.013

Florschuetz, L.W., 1979. Extension of the Hottel-Whillier model to the analysis of combined photovoltaic/thermal flat plate collectors. Sol. Energy 22, 361–366. doi:10.1016/0038-092X(79)90190-7

Hegazy, A.A., 2000. Comparative study of the performances of four photovoltaic / thermal solar air collectors. Energy Convers. Manag. 41.

Hussain, F., Othman, M.Y.H., Yatim, B., Ruslan, H., Sopian, K., Anuar, Z., Khairuddin, S., 2015. An improved design of photovoltaic/thermal solar collector. Sol. Energy 122, 885–891. doi:10.1016/j.solener.2015.10.008

Kaiser, A.S., Zamora, B., Mazon, R., Garcia, J.R., Vera, F., 2014. Experimental study of cooling BIPV modules by forced convection in the air channel. Appl. Energy 135, 88–97. doi:10.1016/j.apenergy.2014.08.079

Kruglov O., Rounis, E.D., Athienitis, A.K., Ge, H., 2017. Experimental investigation and implementation of a multiple-inlet BIPV/T system in a curtain wall. Proceedings of the 15th Canadian Conference on Building Science and Technology (CCBST), Vancouver, 2017.

Rounis, E.D., Kruglov, O., Ioannidis, Z., Athienitis, A.K., Stathopoulos, T., 2017. Experimental investigation of BIPV/T envelope system with thermal enhancements for roof and curtain wall applications. Proceedings of the 34th European PV Solar Energy Conference (EU PVSEC), Amsterdam, 2017.

Skoplaki, E., Palyvos, J.A., 2009. On the temperature dependence of photovoltaic module electrical performance: A review of efficiency/power correlations. Sol. Energy 83, 614–624. doi:10.1016/j.solener.2008.10.008

Tonui, J.K., Tripanagnostopoulos, Y., 2006. Improved PV/T solar collectors with heat extraction by forced or natural air circulation. Int. J. Hydrogen Energy 31, 2137–2146. doi:10.1016/j.ijhydene.2006.02.009

Tonui, J.K., Tripanagnostopoulos, Y., 2007. Air-cooled PV/T solar collectors with low cost performance improvements. Sol. Energy 81, 498–511. doi:10.1016/j.solener.2006.08.002

TESSLibs 17, Component libraries for the TRNSYS simulation environment. Vol. 3, Electrical library mathematical reference.

Wolf, M., 1976. Performance analyses of combined heating and photovoltaic power systems for residences. Energy Convers. 16, 79–90. doi:10.1016/0013-7480(76)90018-8

Yang, T., Athienitis, A.K., 2016. A review of research and developments of building-integrated photovoltaic/thermal (BIPV/T) systems. Renew. Sustain. Energy Rev. 66, 886–912. doi:10.1016/j.rser.2016.07.011

Yang, T., Athienitis, A.K., 2014. A study of design options for a building integrated photovoltaic/thermal (BIPV/T) system with glazed air collector and multiple inlets. Sol. Energy 104, 82–92. doi:10.1016/j.solener.2014.01.049

Zogou, O., Stapountzis, H., 2011. Energy analysis of an improved concept of integrated PV panels in an office building in central Greece. Appl. Energy 88, 853–866. doi:10.1016/j.apenergy.2010.08.023